ELSEVIER

Polymer 43 (2002) 3717–3725

polymer

www.elsevier.com/locate/polymer

Bridged double percolation in conductive polymer composites: an electrical conductivity, morphology and mechanical property study

Wiriya Thongruang[a,1], Richard J. Spontak[a,b], C. Maurice Balik[a,*]

[a]Department of Materials Science and Engineering, North Carolina State University, Raleigh, NC 27695-7907, USA
[b]Department of Chemical Engineering, North Carolina State University, Raleigh, NC 27695-7905, USA

Received 5 November 2001; received in revised form 12 February 2002; accepted 18 February 2002

Abstract

Conductive polymer composites are ubiquitous in technological applications and constitute an ongoing topic of tremendous commercial interest. Strategies developed to improve the level of electrical conductivity achieved at a given filler concentration have relied on double-percolated networks induced by immiscible polymer blends, as well as mixtures of fillers in a single polymer matrix, to enhance interparticle connectivity. In this work, we combine these two strategies by examining quaternary composites consisting of high-density polyethylene (HDPE), ultrahigh molecular weight polyethylene (UHMWPE), graphite (G) and carbon fiber (CF). On the basis of our previous findings, we examine the electrical conductivity, morphology, thermal signature and mechanical properties of HDPE/UHMWPE/G systems that show evidence of double percolation. Upon addition of CF, tremendous increases in conductivity are realized. The mechanism by which this increase occurs is termed *bridged double percolation* to reflect the role of CF in spanning non-conductive regions and enhancing the continuity of conductive pathways. At CF concentrations above the percolation threshold concentration, addition of G promotes increases in conductivity and dynamic storage modulus in which the conductivity increases exponentially with increasing modulus. © 2002 Elsevier Science Ltd. All rights reserved.

Keywords: Polyethylene; Conductive polymer composites; Graphite

1. Introduction

Conductive polymer composites (CPCs) typically consist of a polymeric matrix into which a carbonaceous filler is incorporated. These multifunctional materials are routinely employed in various commercial applications due to their good electrical conductivity, light weight, corrosion resistance and enhanced mechanical properties. Examples of applications that use CPCs include battery and fuel cell electrodes, as well as anti-static and corrosion-resistant materials. Common conductive fillers of current technological relevance include carbon black (CB), graphite (G) and carbon fiber (CF). While the utility of CPCs is well-established, a new generation of efficient CPCs composed of different polymers/fillers and possessing (i) a low percolation threshold concentration (PTC) and (ii) high electrical conductivity continues to be sought. The principal objective of efforts in this vein is to optimize application properties with regard to processability and cost. Processing and associated economic challenges arising from the addition of large quantities of solid fillers to polymeric media have, however, thwarted the development of CPCs. Factors such as the size, shape, chemistry and aggregation behavior of filler particles [1] must be considered in conjunction with the thermodynamic and rheological properties of the polymer matrix [2] and the processing conditions employed [3,4]. Ongoing attempts to localize filler particles at the interface or within one of the phases of an immiscible polymer blend have demonstrated [5–7] that the PTC can be substantially reduced in this manner for a given filler.

While several previous studies [8–12] have used this strategy to reduce the PTC of CB in a variety of polymer blends, we now turn our attention to immiscible blends in which one of the components is high-density polyethylene (HDPE). Due to melt-viscosity differences, CB particles tend to reside predominantly within the HDPE phase, which consequently promotes a substantial reduction in the PTC of CB relative to comparable CPCs produced from either constituent polymer [13–16]. Chan et al. [17] have also considered neat ultrahigh molecular weight polyethylene (UHMWPE) as a matrix polymer for CPCs. In

---

* Corresponding author. Tel.: +1-919-515-2126; fax: +1-919-515-7724.
E-mail address: balik@ncsu.edu (C.M. Balik).

[1] Present address: Department of Mechanical Engineering, Prince of Songkhla University, Songkhla 90112, Thailand.

0032-3861/02/$ - see front matter © 2002 Elsevier Science Ltd. All rights reserved.
PII: S0032-3861(02)00180-5

marked contrast to CPCs derived solely from CB in HDPE, however, the high melt viscosity of UHMWPE effectively forces CB particles to locate almost exclusively along the interface that develops when individual polymer particles are fused together in the melt state. As in immiscible polymer blends, this method of incorporating CB into a polymeric medium results in a reduced PTC. Similarly, addition of CB particles to blends of UHMWPE and low-molecular-weight polyethylene (LMWPE) yields ternary CPCs wherein the CB particles disperse only in the low-viscosity LMWPE phase [18]. Mamunya [19] has proposed that CB, as well as other conductive particles, can be forced to segregate in polymer blends if the particles either reside (as a random distribution) within one of the blend components prior to mixing or migrate to the polymer–polymer interface after mixing.

Previous studies of immiscible polymer blends filled with CB have not only focused on improving electrical conductivity, but have also investigated the corresponding variations that arise in mechanical property development and fabrication [16,20–22]. Other fillers, such as G and CF, have likewise received similar attention in the ongoing development of CPCs. Several different polymer blends composed of HDPE filled with CF have been examined by Zhang et al. [23–25]. They have shown that the conductivity of such ternary CPCs can be enhanced through *double percolation*, which refers to the percolation of CF in the HDPE phase and the continuity of the CF-filled HDPE phase in the polymer blend. They also report that the dispersion of CF depends on the volume fraction of filler and process parameters such as time and temperature. We have recently observed [16] double percolation behavior in immiscible HDPE/UHMWPE blends filled with either CB or G. In the case of each filler, the electrical conductivity and dynamic mechanical properties improve markedly as the concentration of UHMWPE in the blends increases (up to about 80 wt%). On the basis of morphological evidence, these results are interpreted to indicate that continuous HDPE channels filled with percolated filler particles form in UHMWPE-rich blends. More modest increases in electrical conductivity and mechanical properties are observed in HDPE/UHMWPE blends filled with CF due to the large size of the CF particles relative to that of the phase domains comprising the blends.

In a separate study [26], we have also found that mixtures of conductive fillers (e.g. G and CF) in a single polymer matrix can be used to enhance the electrical conductivity and dynamic mechanical properties of CPCs. This observation reflects an overall improvement in the conductive pathway established by particles differing in size and shape. Thus far, we are unaware of any reports that combine, in synergistic fashion, the approaches of blend-induced double percolation and mixture-induced *interparticle bridging* in the rational design of quaternary CPCs. The present study investigates the electrical conductivity, morphology, thermal signature and mechanical properties of HDPE/UHMWPE blends filled with mixtures of G and CF. These components have been selected to permit direct comparison with our previous reports of CPCs prepared with either (i) HDPE and filler mixtures or (ii) HDPE/UHMWPE blends containing a single filler. While comparable CPCs modified with CB are of equal interest in this vein, they are excluded here due to processing difficulties.

2. Experimental

2.1. Materials

The HDPE and UHMWPE polymers used here were received as powders from Celanese. The weight-average molecular weight, mass density, melting temperature and particle size range of the HDPE were <200 kg/mol, 0.964 g/cm^3, 133 °C and 30–90 μm, respectively. The corresponding characteristics of the UHMWPE (GUR-4130) were 3000–5000 kg/mol, 0.930 g/cm^3, 133 °C and 100–150 μm, respectively. The G (#4424) powder with a density of 2.24 g/cm^3 and an aggregate size of about 40 μm was obtained from Asbury. Chopped CF (#34-700) derived from polyacrylonitrile was purchased from Goodfellow. It had a diameter of 7.0 μm, a density of 1.77–1.80 g/cm^3 and a length of 760 μm [26]. Its volume resistivity was reported as 1.5×10^{-3} Ω cm.

2.2. Methods

Powders of as-received HDPE and UHMWPE were first dry-mixed in a mechanical mixer prior to the addition of G, CF or G/CF mixtures. Upon addition of these fillers, each polymer/filler mixture was further dry-mixed to achieve a reasonably uniform dispersion. This mixture was then evenly spread in a 40×120 mm^2 rectangular metal mold, which was subsequently placed in a Carver hydraulic press (Model-C) and heated at ~10 °C/min to temperatures between 160 and 190 °C. At these temperatures, 7.2 MPa of pressure was applied to the mixture for 3 min to ensure complete melting of both polymers. The mold was then cooled at ~20 °C/min by circulating cold water through the platens to inhibit polymer migration. Composite films measuring 0.2–0.8 mm thick and having a maximum filler-mixture loading level of 60 wt% G and 15 wt% CF were obtained by this process. Composite films containing higher concentrations of filler mixture were not uniform and consequently excluded from this study.

The electrical resistivity of CPC films cut to 40×40 mm^2 was measured at ambient temperature by the four-point probe technique (Veeco 5000). The output was subsequently corrected for sample geometry. The average resistivity of each sample was obtained from seven repeated measurements at different locations on the sample, and was then converted to an average conductivity for reporting purposes. The spatial distribution of the G/CF mixture in several HDPE/UHMWPE blends was determined by

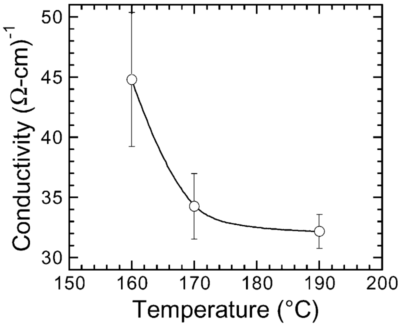

Fig. 1. Conductivity presented as a function of molding temperature for three composites prepared with 35 wt% $\mathrm{PE}_{\mathrm{bl}}^{(2)}$, 50 wt% G and 15 wt% CF. In all cases, the molding time is 3 min. The solid line is a guide for the eye, and the error bars denote one standard error in the data.

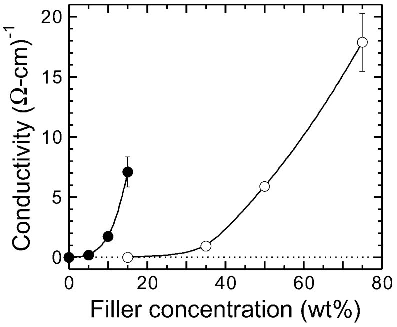

Fig. 2. Dependence of conductivity on filler concentration for composites derived from $\mathrm{PE}_{\mathrm{bl}}^{(2)}$ and containing either G (○) or CF (●). The solid lines serve as guides for the eye, and the error bars denote one standard error in the data.

reflection optical microscopy (BX-60, Olympus). Images of polished sample surfaces (in contact with the metal mold) were acquired with a digital camera (Spot RT, Diagnostic Instrument). The effects of the G/CF mixture on the thermal characteristics of the polymer blend—e.g. melting and crystallization temperatures (T_m and T_c, respectively), specific heat of fusion (Δh_f) and overall crystallinity—were measured by differential scanning calorimetry (DSC). The calorimeter (DSC-7, Perkin–Elmer) was operated at heating and cooling rates of 20 °C/min. Crystallinities were ascertained from the ratio of the measured Δh_f to Δh_f corresponding to 100% crystalline polyethylene (245.3 J/g [27]). The mechanical properties of these quaternary CPCs were investigated by dynamic mechanical analysis (DMA) performed on a DMA 983 (TA Instruments). In these tests, the dynamic storage and loss shear moduli (G' and G'', respectively), as well as tan δ ($=G''/G'$), were evaluated as functions of temperature at small strain amplitudes and a fixed frequency of 1.0 Hz in the linear viscoelastic limit. Specimens measuring $13 \times 40 \times 0.5$ mm^3 were annealed at 90 °C for 60 min prior to DMA and DSC analyses to ensure removal of residual stresses arising from molding.

3. Results and discussion

Since the CPCs of interest here are composed of four different components, namely, HDPE, UHMWPE, G and CF, a small subset of the total specimen matrix must be identified for feasibility purposes. Part of the subset is mandated on the basis of CPC processability (as discussed in Section 2.2). Additional insight into specimen choice can be gleaned from prior experimental findings. Ternary CPCs based on HDPE/UHMWPE blends containing either CB or G exhibit conductivity maxima at blend compositions near 80 wt% UHMWPE. Therefore, it is sensible to select one of the HDPE/UHMWPE blends near this composition for investigation in the present study. In addition to examining CPCs composed of HDPE as the reference material (in which G and CF distribute uniformly), we also elect to choose an intermediate blend composition to facilitate comparison. Composite films consisting of HDPE, 50/50 and 25/75 w/w HDPE/UHMWPE blends and filled with mixtures of G and CF are reproducible (within acceptable experimental error) in terms of their measured properties and are selected here for detailed analysis. For the sake of brevity, the 50/50 w/w HDPE/UHMWPE blend is hereafter referred to as $\mathrm{PE}_{\mathrm{bl}}^{(1)}$, whereas the 25/75 w/w HDPE/UHMWPE blend is denoted $\mathrm{PE}_{\mathrm{bl}}^{(2)}$. In addition to CPC composition, variation in process conditions must also be considered to achieve CPC reproducibility. Molding temperatures ranging from 160 to 190 °C have been used to prepare CPCs filled with G/CF mixtures. According to the electrical conductivity data presented in Fig. 1 for $\mathrm{PE}_{\mathrm{bl}}^{(2)}$, this process variable significantly affects CPC property development and reproducibility. In contrast, the molding time at 190 °C has little effect on conductivity (data not shown). Thus, molding is conducted at 190 °C for 3 min throughout the remainder of this study.

3.1. Electrical conductivity

Fig. 2 provides the electrical conductivity of CPCs based on $\mathrm{PE}_{\mathrm{bl}}^{(2)}$ as a function of either G or CF loading level. The first datum point in each data set identifies no conductivity, whereas the second point corresponds to non-zero conductivity near the PTC. These data clearly show that the PTC of the CPCs containing CF is substantially lower than that of the CPCs with G. Moreover, conductivity is observed to be more strongly dependent on filler concentration in the CF-based CPCs than in the G-based materials. This composition sensitivity is attributed to the size of the CF particles, which are considerably longer than the G particles and which are more likely to form continuous conductive pathways within the polymer blend. Conductivity measurements acquired from the quaternary CPCs of principal interest in the present work are displayed as a function of filler content in Fig. 3 for HDPE, $\mathrm{PE}_{\mathrm{bl}}^{(1)}$ and $\mathrm{PE}_{\mathrm{bl}}^{(2)}$ containing 15 wt% CF and varying concentrations of G. Note that CPCs composed of neat UHMWPE are excluded from this comparison due to their

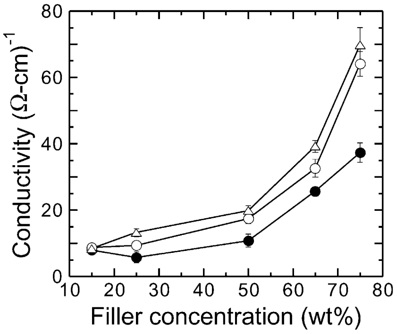

Fig. 3. Variation of conductivity with total filler concentration for HDPE (●), $\mathrm{PE}_{\mathrm{bl}}^{(1)}$ (○) and $\mathrm{PE}_{\mathrm{bl}}^{(2)}$ (△) composites containing mixtures of G and CF. In all cases, the concentration of CF accounts for 15 wt% of the composite. The solid lines serve to connect the data, and the error bars denote one standard error in the data.

typically low conductivity [16]. Since the convention by which we designate composition in these quaternary CPCs is important, we provide an example of how to analyze the data shown in this figure. Consider a CPC composed of $\mathrm{PE}_{\mathrm{bl}}^{(2)}$ with 60 wt% filler. This system consists of 15 wt% CF, 45 wt% G and 40 wt% polymer, the latter of which can be further divided into its blend components—10 wt% HDPE and 30 wt% UHMWPE.

As anticipated from Fig. 2, an increase in filler concentration is generally accompanied by an increase in electrical conductivity due to greater interparticle contact. Comparison of the data in Figs. 2 and 3 reveals that CPCs prepared from neat HDPE and mixtures of G and CF exhibit significantly higher conductivity than CPCs derived from $\mathrm{PE}_{\mathrm{bl}}^{(2)}$ in the presence of only G. At 75 wt% filler, for instance, the conductivity of the $\mathrm{PE}_{\mathrm{bl}}^{(2)}$/G composite is about 18 $(\Omega\ \mathrm{cm})^{-1}$, whereas that of the HDPE/G/CF composite is about 37 $(\Omega\ \mathrm{cm})^{-1}$. Addition of 15 wt% CF to 60 wt% G therefore accounts for more than a 100% increase in conductivity. By incorporating UHMWPE into these CPCs, the conductivity can be further improved, as evidenced by the data obtained from the $\mathrm{PE}_{\mathrm{bl}}^{(1)}$- and $\mathrm{PE}_{\mathrm{bl}}^{(2)}$-based CPCs in Fig. 3. If we again consider the CPCs with 75 wt% filler, we see that the conductivity increases from 37 to 64–69 $(\Omega\ \mathrm{cm})^{-1}$ as the UHMWPE content increases from 0 to 50–75 wt%. Over this composition interval under constant filler conditions, the electrical conductivity increases by 1.5–2.2 × over the entire range of filler concentrations examined. The results provided in Figs. 2 and 3 also indicate that substitution of 15 wt% CF for G in the $\mathrm{PE}_{\mathrm{bl}}^{(2)}$/G composite promotes a considerable increase in electrical conductivity (by about 280% at 75 wt% filler content).

It is interesting to note that the conductivity increases evident in Fig. 3 become more pronounced at mixed filler concentrations above 50 wt%. At this concentration, the CPCs consist of 35 wt% G and 15 wt% CF. According to the conductivity measurements provided in Fig. 2 and detailed elsewhere [16], the PTC of G in $\mathrm{PE}_{\mathrm{bl}}^{(2)}$ is approximately 35 wt%. In neat HDPE, this PTC occurs at closer to 50 wt% G [26]. Thus, the PTC of G can be controllably lowered through judicious choice of blend components and composition in a CPC. In marked contrast, the PTC of CF is relatively independent of composition in the HDPE/UHMWPE system, varying from about 5.0 wt% in neat HDPE to 7.5 wt% in $\mathrm{PE}_{\mathrm{bl}}^{(2)}$. At 15 wt%, CF is above its PTC in all the CPCs discussed with regard to the conductivity measurements in Fig. 3. Two issues must therefore be addressed to elucidate the mechanism by which conductivity is improved in these systems. The first is the role of the UHMWPE in the polymer blends, and the second is the CF loading level. Addition of UHMWPE to HDPE results in transient phase segregation due to a substantial difference in melt viscosity [28]. An increase in UHMWPE content therefore promotes the formation of UHMWPE- and HDPE-rich regions, as schematically depicted in Fig. 4(a). If the matrix consists of HDPE, both G and CF at a given filler concentration are anticipated to remain isotropically distributed within the low-viscosity HDPE phase. In this case, the purpose of the CF is to bridge distant and unconnected G particles, thereby increasing the net conductivity of the composite.

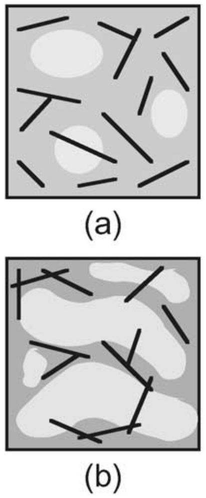

Fig. 4. Schematic diagram showing the effect of polymer blend composition on filler connectivity. If one phase (A, gray) of an immiscible blend possesses a higher melt viscosity than the other (B), G and CF particles will locate in B (a). As the fraction of A increases (b), the G/CF mixture becomes constrained within channels of B, eventually forming a bridged double-percolated network. In this case, discrete G-rich channels of B are connected by CF particles.

As the composition of UHMWPE increases, however, the HDPE is arranged into continuous channels that remain filled with G particles. This leads to the formation of a double-percolated network [8,16,23–25,29,30], which is shown in Fig. 4(b). Such localization of filler particles induces an enormous increase in conductivity. As alluded to earlier, double percolation occurs up to about 80 wt% in the HDPE/UHMWPE blend system. At this blend composition, a conductivity maximum is observed [16] in the case of CB and G fillers. At higher UHMWPE concentrations,

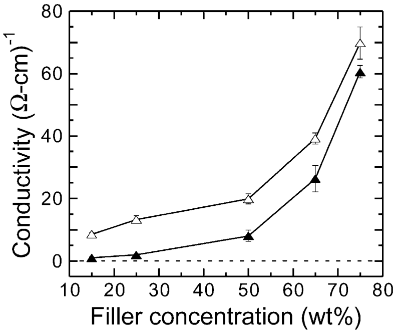

Fig. 5. Conductivity presented as a function of total filler concentration for $\mathrm{PE}_{\mathrm{bl}}^{(2)}$-based composites containing mixtures of G and CF at two different loading levels of CF (expressed as wt% of the composite): 5 (▲) and 15 (△). The solid lines serve to connect the data, and the error bars denote one standard error in the data.

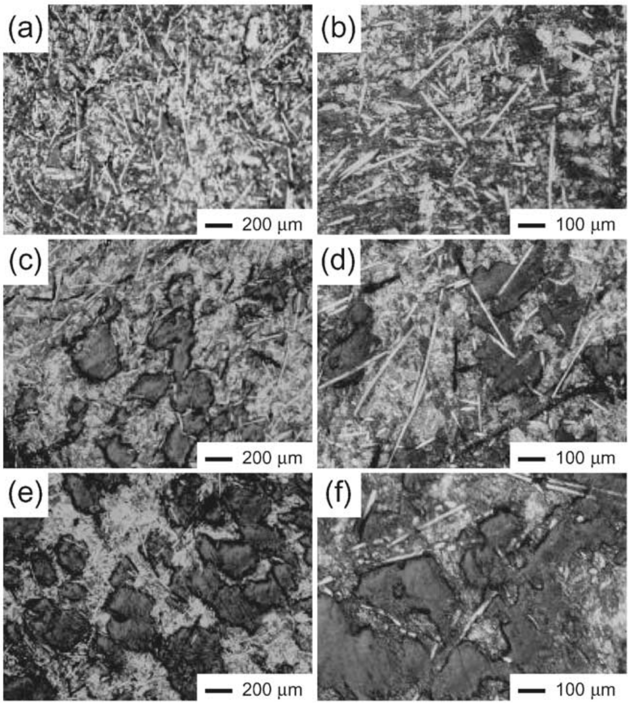

Fig. 6. Low- and high-magnification optical micrographs obtained from composites produced with 50 wt% G, 15 wt% CF and 35 wt% of the following polymeric constituents: (a,b) HDPE, (c,d) $\mathrm{PE}_{\mathrm{bl}}^{(1)}$ or (e,f) $\mathrm{PE}_{\mathrm{bl}}^{(2)}$. These images have been acquired in reflection mode from polished specimen surfaces.

conductive pathways are obstructed and CPC conductivity decreases as the HDPE-rich regions eventually become isolated. This model explains how the composition of the polymer blend comprising a CPC impacts conductivity, but does not address how the mixed G/CF filler promotes the tremendous conductivity increases evident in Fig. 3. Since the CF particles are substantially longer than the particle sizes of HDPE and UHMWPE, we anticipate that, at high UHMWPE concentrations, the CF can span UHMWPE-rich domains and connect G-rich HDPE domains that may not be otherwise connected. This postulated scenario is shown in Fig. 4(b) and suggests that the CF particles not only bridge G particles within single HDPE channels, but also bridge G particles residing in neighboring channels, thereby promoting more conductive pathways through the composite medium. We therefore refer to this mechanism as bridged double percolation to reflect the requirements of (i) double percolation and (ii) interchannel connectivity.

Since double percolation (and, by logical inference, bridged double percolation) is most pronounced in CPCs derived from $\mathrm{PE}_{\mathrm{bl}}^{(2)}$, we focus our attention on this system for the remainder of this study. Another consideration in the design of CPCs based on bridged double percolation is the role of CF concentration. As mentioned earlier, CF at 15 wt% is above its PTC and promotes electrical conductivity and mechanical stability [26]. Fig. 5 displays conductivity data acquired from $\mathrm{PE}_{\mathrm{bl}}^{(2)}$ filled with 5 and 15 wt% CF and varying levels of G. At low mixed filler concentrations, the conductivity level of the CPCs with 5 wt% CF is not far removed from the PTC of the system (i.e. near zero conductivity). Beyond 50 wt% filler, however, the conductivities of the CPCs with 5 and 15 wt% CF are both found to increase sharply. Over the entire filler concentration range examined here, the conductivities of the CPCs with 5 wt% CF are generally less than those of the composites with 15 wt% CF. This observation is consistent with the bridged double percolation model depicted in Fig. 4. In the event that no CF is added to $\mathrm{PE}_{\mathrm{bl}}^{(2)}$ (Fig. 2), the maximum conductivity achieved at any given filler loading level directly reflects the conductive pathways established solely by contacted filler particles in continuous HDPE channels. To achieve greater conductivity, CF particles must be present to ensure that the G particles in neighboring channels are physically connected even though the channels are not.

3.2. Morphological characteristics

Since the fillers employed here are relatively large, we expect that the bridged double percolation model proposed here can be corroborated by examining the morphologies of the quaternary CPCs discussed with regard to Fig. 3. Optical micrographs acquired in reflection mode of polished CPCs composed of 35 wt% polymer and 65 wt% filler (50 wt% G and 15 wt% CF) are displayed for different blend compositions in Fig. 6. If the polymer matrix is neat HDPE (Figs. 6(a) and (b)), the G and CF particles, which appear as bright features set against a dark polymer-rich background, are observed to be uniformly and isotropically distributed. Note, however, the existence of relatively large gaps between some of the particles. These gaps, most likely due to the presence of HDPE spherulites, reduce the degree of contact between neighboring particles and, hence, the net conductivity of the HDPE/G/CF composite. Once UHMWPE is introduced into these CPCs, the particles adopt a more selective, anisotropic spatial arrangement. In the CPCs derived from $\mathrm{PE}_{\mathrm{bl}}^{(1)}$ (Figs. 6(c) and (d)), the G particles localize within continuous regions that are

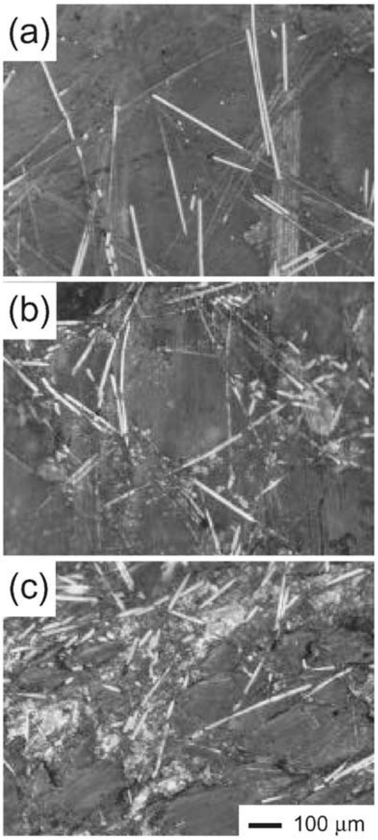

Fig. 7. Optical micrographs of $PE_{bl}^{(2)}$ filled with 15 wt% CF and different concentrations of G (in wt%): (a) 0, (b) 10 and (c) 35. These images have been collected under the same conditions as those shown in Fig. 6.

presumably HDPE-rich, since low-viscosity HDPE can efficiently wet the carbonaceous filler particles and flow around high-viscosity obstacles. While many of the CF particles tend to orient within these regions, some span across polymer-rich (dark) regions that measure on the order of 100–200 μm across. This size scale is consistent with the particle size of the as-received UHMWPE, in which case it is reasonable to designate these regions as UHMWPE-rich. As expected, the G particles do not disperse within these regions due to the high-viscosity of UHMWPE. Figs. 6(c) and (d) confirm that HDPE/UHMWPE blends can undergo transient phase-segregation, which agrees with the previous findings of Vadhar and Kyu [28]. These images also demonstrate that (i) the filler particles selectively localize within the HDPE phase, and (ii) the CF serves to connect G particles residing in the same, as well as in adjacent, channels.

If the UHMWPE content is further increased to 75 wt% of the HDPE/UHMWPE blend (as in Figs. 6(e) and (f)), the HDPE-rich regions become narrower due to greater volumetric constraints, thereby forcing the G and CF particles to pack together more efficiently at constant filler concentration. The presence of CF-induced interchannel connections is clearly visible in these micrographs and further supports the bridged double percolation mechanism introduced earlier. Another interesting point to recognize in this image pair is that the area fraction of UHMWPE-rich regions increases with increasing UHMWPE composition. This observation, which is to be expected for fully immiscible polymer blends, implies that these two polymers, while chemically identical, do not co-crystallize under the conditions employed here, as explained by Sumita et al. [31]. It is important to remember that the highly constrained particles evident in Figs. 6(e) and (f) reflect a CPC at high filler loading. A series of optical micrographs obtained at lower filler concentrations is provided in Fig. 7. In this series, all the CPCs possess 15 wt% CF and levels of G ranging from 0 wt% in Fig. 7(a) to 35 wt% in Fig. 7(c). In Fig. 7(a), the CF particles are randomly oriented in a continuous polymer matrix. While no evidence of phase segregation is discernible in this CPC (which is to be expected since the CF particles are longer than, and less affected by, the high-viscosity UHMWPE domains), large gaps are seen to exist between the CF particles. Addition of 10 wt% G (Fig. 7(b)) is accompanied by the onset of particle localization. As in Fig. 7(a), however, the dispersion of CF particles does not appear to be strongly affected. Note that some of the CF particles reside in close proximity to the G particles. Increasing the G concentration to 35 wt% (Fig. 7(c)) clearly reveals that (i) the G particles localize within the HDPE-rich channels and (ii) CF particles span UHMWPE-rich regions to connect G particles in adjacent HDPE-rich regions.

3.3. Thermal properties

As mentioned earlier, an important consideration in the development of CPCs derived from a semicrystalline polymer blend is the influence of polymer crystals on filler particle dispersion. The converse is likewise true. A solid filler incorporated into the matrix of a semicrystalline polymer may behave as a heterogeneous nucleating agent. To determine if G, CF or G/CF mixtures have any influence on HDPE or UHMWPE crystallization, we next examine the thermal signatures of the polymer blends and CPCs prepared during the course of this study. Table 1 is a compilation of the thermal properties measured from HDPE, UHMWPE and select HDPE/UHMWPE blends in the absence of filler. Within experimental uncertainty, T_m and T_c are virtually independent of blend composition in this series. The crystallinity of the neat HDPE is determined from the measured value of Δh_f to be 85.0%, which is much higher than that of the UHMWPE (45.4%). The crystallinities of the 50/50 and 25/75 w/w HDPE/UHMWPE blends are 65.0 and 56.4%, respectively. It is reassuring that these experimental values are in agreement with crystallinities predicted from the linear rule of mixtures (65.5 and 54.6%, respectively).

Since the melting temperatures of the two polymers are almost identical, it cannot be ascertained from these data alone if HDPE and UHMWPE co-crystallize. While an in-depth analysis of DSC thermograms and light scattering patterns may reveal whether these polymers are capable of

Table 1
Thermal properties of HDPE, UHMWPE and their blends (determined from DSC performed at heating and cooling rates of 20 °C/min)

Specimen	T_m (°C)	T_c (°C)	Δh_f (J/g)	Crystallinity[a] (%)
HDPE	133	107	209	85.0
UHMWPE	133	107	111	45.4
50/50 w/w HDPE/UHMWPE	135	107	160	65.0
25/75 w/w HDPE/UHMWPE	132	107	138	56.4

[a] Calculated from the ratio of the measured Δh_f to Δh_f of a 100% crystalline polyethylene (245.3 J/g [27]).

co-crystallization [32,33], such analysis is beyond the scope of the present study. According to the data provided in Table 2, addition of a mixed filler composed of 50 wt% G and 15 wt% CF to the three polymer systems listed in Table 1 has almost no effect on the thermal properties of the resultant CPCs. These findings, which are consistent with previous results acquired from CPCs consisting of (i) HDPE with mixtures of G and CF [26] and (ii) $\mathrm{PE}_{\mathrm{bl}}^{(2)}$ with either G or CF [16], demonstrate that the carbonaceous fillers examined here do not alter the thermal properties of the parent polymers and their blends. Moreover, these fillers do not induce heterogeneous nucleation in these polyethylene-based CPCs. In similar fashion, Xu et al. [34] have also reported that CB does not affect the thermal behavior of UHMWPE on the basis that the polymer crystal size is independent of the filler loading level.

3.4. Mechanical properties

The dynamic shear moduli (G' and G'') of all the polymer blends and CPCs investigated here have been measured from 25 to 120 °C. Since the storage modulus directly relates to specimen stiffness and mechanical stability, we only discuss the temperature (T) dependence of G' in this section. (The corresponding temperature dependence of G'' does not reveal any notable features and is not included here.) The effect of temperature on G' measured from the neat HDPE and UHMWPE, as well as from $\mathrm{PE}_{\mathrm{bl}}^{(1)}$ and $\mathrm{PE}_{\mathrm{bl}}^{(2)}$, is shown in Fig. 8. In all cases, G' is observed to decrease monotonically with increasing temperature until it reaches a temperature at which it drops precipitously. This temperature, which is associated with the onset of crystal melting or polymer flow, is material-dependent: about 90 °C for HDPE and $\mathrm{PE}_{\mathrm{bl}}^{(1)}$, 98 °C for $\mathrm{PE}_{\mathrm{bl}}^{(2)}$ and 117 °C for UHMWPE. Note that these temperatures are significantly lower than the T_m values reported in Table 1. As expected from the previous DSC results, the $G'(T)$ data provided in Fig. 8 do not exhibit any other thermal transitions, in which case we now turn our attention to the magnitude of G'. Up to ca. 70 °C, G' measured from the four systems discussed earlier lies between 10^8 and 10^9 Pa, with the high-crystallinity HDPE consistently possessing the highest G'. While the values of G' obtained from the two blends fall between those of neat HDPE and UHMWPE, they do not obey the rule of mixtures, which most likely reflects poor mixing [35]. At temperatures just above 70 °C, the relative order in which G' continues to decrease with increasing temperature changes. For instance, $G'(T)$ corresponding to the neat HDPE becomes more sensitive to temperature and decreases more sharply than that of the other systems as it approaches its catastrophic-failure temperature. The data displayed in Fig. 8 reveal that UHMWPE exhibits the greatest thermal stability relative to HDPE and the two blends due to its high degree of chain entanglement (which hinders polymer motion at elevated temperatures).

Table 2
Thermal properties of CPCs composed of HDPE and UHMWPE/HDPE blends (specimens consisted of 35 wt% polymer, 50 wt% G and 15 wt% CF, and were characterized as in Table 1)

Specimen[a]	T_m (°C)	T_c (°C)	Δh_f (J/g)	Crystallinity (%)
HDPE/(G+CF)	135	108	199	81.1
$\mathrm{PE}_{\mathrm{bl}}^{(1)}$/(G+CF)	133	110	159	64.8
$\mathrm{PE}_{\mathrm{bl}}^{(2)}$/(G+CF)	132	105	132	53.8

[a] $\mathrm{PE}_{\mathrm{bl}}^{(1)}$ and $\mathrm{PE}_{\mathrm{bl}}^{(2)}$ refer to the 50/50 and 25/75 w/w HDPE/UHMWPE blends, respectively.

Upon addition of 50 wt% G and 15 wt% CF to HDPE and the two polymer blends discussed with regard to Fig. 8, the magnitude of G' increases by at least 6 ×, as is evident in Fig. 9. The CPC composed of HDPE exhibits the highest G', followed closely by the CPC derived from $\mathrm{PE}_{\mathrm{bl}}^{(1)}$. This order is consistent with the DSC results listed in Table 2, which confirm that polymer crystallinity is unaffected by the addition of the G/CF mixture. Although these filler-induced

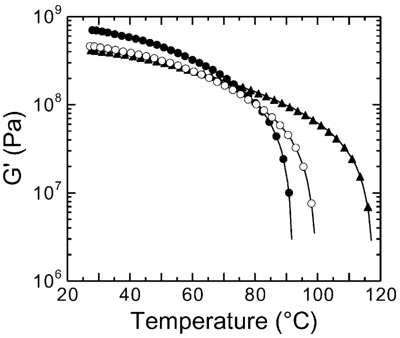

Fig. 8. The dynamic storage modulus (G') displayed as a function of temperature for unfilled HDPE (●), UHMWPE (▲) and $\mathrm{PE}_{\mathrm{bl}}^{(2)}$ (○). Values of G' measured from $\mathrm{PE}_{\mathrm{bl}}^{(1)}$ lie very close to those of neat HDPE and are not included here for that reason. The solid lines serve to connect the data.

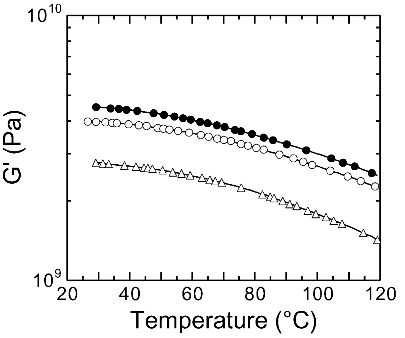

Fig. 9. Temperature dependence of G' for composites containing 50 wt% G, 15 wt% CF and 35 wt% of the following polymeric constituents: HDPE (●), $\mathrm{PE}_{\mathrm{bl}}^{(1)}$ (○) or $\mathrm{PE}_{\mathrm{bl}}^{(2)}$ (△). The solid lines serve to connect the data.

increases in the magnitude of G' are certainly attractive, the most striking feature of the $G'(T)$ data in Fig. 9 is the absence of a temperature at which a steep reduction in G' occurs (as in Fig. 8). Incorporation of the G/CF mixed filler into HDPE and the two HDPE/UHMWPE blends promotes a substantial improvement in the thermal stability of the CPCs to temperatures beyond 120 °C. While this improvement is achieved at a relatively high loading of mixed filler (50 wt% G and 15 wt% CF), it is important to identify the CPC features responsible for such improvement. Fig. 10 shows $G'(T)$ for the $\mathrm{PE}_{\mathrm{bl}}^{(2)}$ blend and its CPCs with varying levels of G and CF. As in Fig. 8, the unfilled blend exhibits a temperature at which G' decreases dramatically. Addition of either G or CF to the blend at a loading level near or above the PTC (35 wt% for G and 5 wt% for CF) yields a ternary CPC that remains thermally stable at much higher temperatures. Mixtures of these fillers (i) maintain thermal stability at temperatures beyond 120 °C and (ii) increase the magnitude of G' over the temperature range explored. Consider, for example, the properties of the CPCs at 30 °C. The value of G' for the unfilled $\mathrm{PE}_{\mathrm{bl}}^{(2)}$ blend at this temperature is about 0.45 GPa. The corresponding values of G' for the ternary CPCs with 35 wt% G or 15 wt% CF are 1.14 and 1.41 GPa, respectively. By combining both fillers at these concentrations to form a quaternary CPC, G' increases to 2.31 GPa, which is surprisingly close to the sum of the G' values (2.55 GPa) obtained from the two ternary systems.

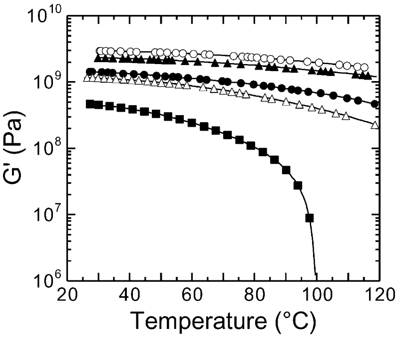

Fig. 10. Variation of G' with respect to temperature for $\mathrm{PE}_{\mathrm{bl}}^{(2)}$ filled with mixtures of G and CF at different concentrations (in w/w G/CF): 0/0 (■), 0/15 (●), 35/0 (△), 35/15 (▲) and 60/15 (○). The solid lines serve to connect the data.

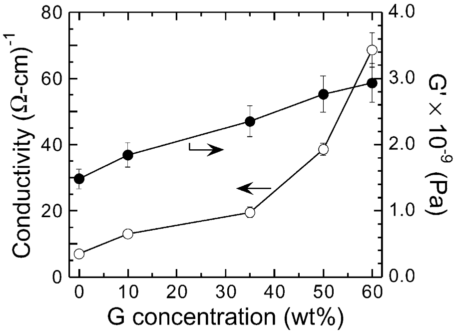

Fig. 11. Dependence of conductivity (○) and G' (●) on G loading in $\mathrm{PE}_{\mathrm{bl}}^{(2)}$ filled with 15 wt% CF. The solid lines connect the data. Error bars on the conductivity data denote one standard error, while those on the G' data represent ±10% uncertainty.

Thus, the mechanical, as well as conductive, properties of quaternary CPCs can be finely tuned by judicious choices of blend and filler composition. While the experimental matrix for quaternary systems precludes systematic variation of all the CPC components employed here, we now focus on establishing the effect of G concentration on the electrical conductivity and mechanical properties of CPCs composed of $\mathrm{PE}_{\mathrm{bl}}^{(2)}$ with 15 wt% CF. These data are presented in Fig. 11. On the basis of the previous findings reported in this work, an increase in the loading level of G is expected to increase both the conductivity and G', which is apparent in this figure. It is interesting to note that the conductivity displays an abrupt increase at the PTC of G (35 wt%). Whereas the G-induced increase in conductivity is significant as it increases by an order of magnitude from 6.9 $(\Omega\ \mathrm{cm})^{-1}$ at 0 wt% G to 69 $(\Omega\ \mathrm{cm})^{-1}$ at 60 wt% G, the corresponding increase in G' is relatively modest. These measurements reveal that once a filler is percolated in a CPC (recall that, at 15 wt%, CF is above its PTC), incorporation of additional filler material strongly impacts the conductivity by establishing more conductive pathways. Since a reinforcing network is already in place, however, the additional filler has less effect on the mechanical properties of the CPC. The data provided in Fig. 11 can be cross-plotted, as in Fig. 12, to yield conductivity as an explicit function of G'. This relationship reveals an unexpected result, namely, that the conductivity increases exponentially (denoted by the solid line in Fig. 12) with respect to G' in the quaternary CPCs used to generate Fig. 11. Thus, a small increase in G' is accompanied by a rather significant increase in electrical conductivity.

4. Conclusions

Conductive polymer composites remain an important topic in the development of new and efficient multifunctional materials. Numerous studies have previously

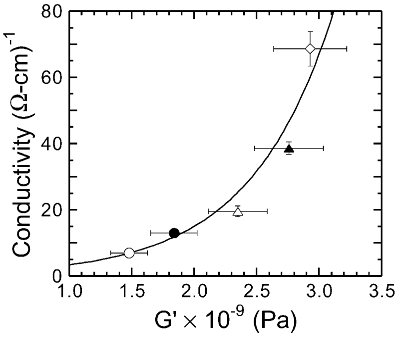

Fig. 12. Conductivity shown as a function of G' for the same systems displayed in Fig. 11. The concentrations of G (in wt%) are 0 (○), 10 (●), 35 (△), 50 (▲) and 60 (◇). The solid line is an exponential fit to the data. The error bars are described in the caption of Fig. 11.

established the importance of polymer–polymer miscibility in the presence of a single carbonaceous filler, as well as the utility of using mixed fillers in the presence of a single polymer. In this work, we have combined these two design strategies—a phase-segregated polymer blend and a mixture of fillers—to develop novel quaternary composite materials composed of HDPE, UHMWPE, G and CF. On the basis of electrical conductivity measurements, we have proposed the concept of a bridged double percolation network. In this model, one filler (e.g. G) is selectively located and percolated within a polymer phase that forms continuous channels and is itself percolated throughout the blend. The purpose of the second filler (e.g. CF) is to span across insulating regions and further connect existing conductive pathways. In this manner, the second filler serves to bridge the double-percolated network and enhance the net conductivity of the composite. This model is consistent with optical micrographs obtained from composites differing in blend and filler composition. These factors also affect the mechanical properties of such composites. Once the PTC of either filler is reached, the dynamic storage modulus of these quaternary composites becomes less temperature-dependent and remains stable up to 120 °C, which is about 30 °C higher than the temperature at which the modulus of HDPE drops precipitously (due to the onset of crystal melting or polymer flow). At these filler concentrations, further addition of filler results in a substantial increase in electrical conductivity, but a modest increase in modulus. Under the conditions examined here, we find that conductivity increases exponentially with increasing modulus. The mechanisms and relationships identified in this work are anticipated to expedite the rational design of multicomponent CPCs, as well as promote an improved understanding of how the properties of commodity materials can be best utilized to achieve application requirements.

Acknowledgements

We thank Mr A. Rieves (National Power American Technology, Inc.) for providing the HDPE and graphite powder, and Drs R.F. Davis, T. Hare, D.M. Maher (NCSU) and K.C. Caster (Lord Corporation) for technical assistance.

References

[1] Calberg C, Blacher S, Gubbels F, Brouers F, Deltour R, Jérôme R. J Phys D: Appl Phys 1999;32:1517.
[2] Miyasaka K, Watanabe K, Jojima E, Aida H, Sumita M, Ishikawa K. J Mater Sci 1982;17:1610.
[3] Huang JC, Wu CL, Grossman SJ. J Polym Eng 2000;20:213.
[4] Hopkins AR, Reynolds JR. Macromolecules 2000;33:5221.
[5] Gubbels F, Jérôme R, Teyssié R, Vanlathem E, Deltour R, Calderone A, Parenté V, Brédas J. Macromolecules 1994;27:1972.
[6] Gubbels F, Blacher S, Jérôme R, Deltour R, Brouers F, Teyssié P. Macromolecules 1995;28:1559.
[7] Gubbels F, Jérôme R, Vanlathem E, Deltour R, Blacher S, Brouers F. Chem Mater 1998;10:1227.
[8] Tchoudakov R, Breuer O, Narkis M, Siegmann A. Polym Eng Sci 1996;36:1336.
[9] Tang H, Chen XF, Tang AQ, Luo YX. J Appl Polym Sci 1996;59:383.
[10] Zhang XW, Huang R, Cai BH, Lai SM, Fan WY. Prog Natl Sci 1996;6:346.
[11] Breuer O, Tchoudakov R, Narkis M, Siegmann A. J Appl Polym Sci 1999;73:1655.
[12] Cheah K, Forsyth M, Simon GP. J Polym Sci B: Polym Phys 2000;38:3106.
[13] Asai S, Hayakawa Y, Suzuki K, Sumita M. Kobunshi Ronbunshu 1991;48:635.
[14] Zhang C, Han HF, Yi XS, Asai S, Sumita M. Compos Interf 1999;6:227.
[15] Feng JY, Chan CM. Polym Eng Sci 1998;38:1649.
[16] Thongruang W, Balik CM, Spontak RJ. J Polym Sci B: Polymer Phys, in press.
[17] Chan CM, Cheng CL, Yuen MMF. Polym Eng Sci 1997;37:1127.
[18] Bin Y, Xu C, Agari Y, Matsuo M. Colloid Polym Sci 1999;277:452.
[19] Mamunya YP. J Macromol Sci, Phys 1999;B38:615.
[20] Yi XS, Wu CZ, Ma DL. J Appl Polym Sci 1998;67:131.
[21] Foulger SH. J Appl Polym Sci 1999;72:1573.
[22] Breuer O, Tzur A, Narkis M, Siegmann A. J Appl Polym Sci 1999;74:1731.
[23] Zhang C, Yi XS, Yui H, Asai S, Sumita M. J Appl Polym Sci 1998;69:1813.
[24] Zhang C, Yi XS, Yui H, Asai S, Sumita M. Mater Lett 1998;36:186.
[25] Zhang C, Yi XS, Asai S, Sumita M. Compos Interf 1999;6:287.
[26] Thongruang W, Spontak RJ, Balik CM. Polymer 2002;43:2279.
[27] Brandrup J, Immergut EH, Grulke EA, editors. Polymer handbook. 4th ed. New York: Wiley, 1999.
[28] Vadhar P, Kyu T. Polym Eng Sci 1987;27:202.
[29] Foulger SH. J Polym Sci 1999;37:1899.
[30] Feng J, Chan CM. Polymer 2000;41:4559.
[31] Sumita M, Sakata K, Asai S, Miyasaka K, Nakagawa H. Polym Bull 1991;25:265.
[32] Kyu T, Vadhar P. J Appl Polym Sci 1986;32:5575.
[33] Tinçer T, Coskun M. Polym Eng Sci 1993;33:1243.
[34] Xu C, Agari Y, Matsuo M. Polym J 1998;30:372.
[35] Bhateja SK, Andrews EH. Polym Eng Sci 1983;23:888.